EEG Correlates of Submovements

L. Dipietro, H. Poizner, and H.I. Krebs, *Senior Member, IEEE*

Abstract—**Numerous studies on motor control in humans and primates have suggested that the Central Nervous System (CNS) generates and controls continuous movement via discrete, elementary units of movement or submovements. While most studies are based on analysis of kinematic data, investigations of neural correlates have been lacking. To fill this gap we recorded and analyzed kinematic and high-density electroencephalographic (64-channel EEG) data from three right-handed normal adults during a reaching task that required online movement corrections. Each kinematic submovement was accompanied by stereotyped scalp maps. Furthermore, the peaks of event-related potentials (ERP) recorded at electrode C1 (over contralateral motor cortex) were time-locked to kinematic submovement peaks. These results provide further evidence for the hypothesis that the CNS generates and controls continuous movement via discrete submovements. Applications include design of quantitative outcome metrics for motor disorders of neurological origin such as stroke and Parkinson's disease.**

I. INTRODUCTION

A key feature of the motor system is the ability to correct movement online as unexpected changes in the motor task specifications arise. To this end, the CNS must be able to modify ongoing motor commands, but the exact mechanisms underlying such process remain unclear. Several studies have suggested submovements or elementary units of movement as a possible mechanism used by the CNS to generate complex motor behavior, including online corrections. According to this hypothesis, the CNS does not control *continuous* movement in a *continuous* fashion but rather via generating and combining *discrete* elements whose features (e.g. amplitude and duration) can be modulated depending on the motor task. Submovements have been observed in a variety of motor tasks, including reaching under accuracy constraints [1] [2] [3] [4], handwriting [5], learning of new motor tasks [6] [7] [8] and are particularly evident in movements performed by stroke patients during the early phase of recovery [7]. While most

studies have focused on analysis of kinematic data, investigations of neural correlates of kinematic submovements have been sparse. This study is part of a series of studies by our group aimed at understanding neural mechanisms underlying submovements for the purpose of designing more effective robot-assisted neurorehabilitation treatments where the therapeutic action is controlled by patient's motor intentions [8] [9] [10] and for enhancing our understanding of the neural control of movement [11] [12] [13]. Here we sought to explore whether a signature of submovements can be found in EEG by simultaneously recording EEG and kinematic data from healthy subjects during a double step target displacement task [14] [15] which is known to evoke online corrections of movement trajectories. We hypothesized that if submovements have a discrete nature, then underlying neural activity as recorded by EEG should also be characterized by stereotyped spatio-temporal features, time-locked to features of kinematic submovements.

II. MATERIALS AND METHODS

A. Hardware

An InMotion3 wrist robot (Interactive Motion Technologies, Watertown, MA) designed for clinical neurological applications, was used in this study. The robot had 3 actuated degrees-of-freedom, namely radial/ulnar deviation, flexion/extension, and pronation/supination. A complete description of the hardware is reported in [16]. The angular positions were acquired digitally (sampling frequency f_s = 1000 Hz, 16-bit quantization).

EEG was recorded continuously with a sampling rate of 1024 Hz using a 64-channel Active-Two EEG system (BioSemi, Amsterdam, the Netherlands).

Figure 1: Experimental set-up.

B. Experimental Procedure

Three healthy, right-handed subjects (age 25.3±5.5 years) with no history of neurological disorders participated in this experiment. Experiments were approved by MIT's Committee on the Use of Humans as Experimental Subjects and by the Institutional Review Board of UCSD. Informed written consent was obtained from all subjects.

L. D. is with the Massachusetts Institute of Technology, Mechanical Engineering Department, Cambridge, MA 02139 USA (phone: 617-253-8114; fax: 617-258-7018; e-mail: lauradp@ mit.edu).

H. P. is with University of California, San Diego, Institute for Neural Computation, Department of Cognitive Science and Program in Neurosciences, La Jolla, CA 92093 USA (e-mail: hpoizner@ucsd.edu).

H. I. K. is with the Massachusetts Institute of Technology, Mechanical Engineering Department, Cambridge, MA 02139 USA and University of Maryland School of Medicine, Neurology Department, Baltimore, MD 21201(e-mail: hikrebs@mit.edu). H.I.K. is a co-inventor in MIT-held patent for the robotic device used here. He holds equity positions in Interactive Motion Technologies, Inc., the company that manufactures this type of technology under license to MIT.

Subjects were comfortably seated in front of a computer screen and held the handle of the wrist robotic device in their right hand (Figure 1). Velcro straps at the upper arm and distal forearm minimized arm movement. The screen displayed 8 outer targets (diameter 2.5 cm) placed on a circle and a central target. Outer targets were presented in a pseudo-random order and the central target was presented following presentation of an outer target. Subjects were instructed to move the handle of the robot to make the cursor reach the target that was presented. The motor task required wrist flexion/extension and radial/ulnar deviation (30 and 15 degrees rotation). The amount of subjects' wrist rotation was mapped to the position of a cursor also shown on the screen. The maximum time allotted for movement from the central target to an outer target or from an outer target to return was 1.4 seconds. At time t=0 one of the outer targets was illuminated on the screen. The outer target might remain lit (*control condition*) or shift mid-movement to another target requiring a movement correction (*shift condition*). Targets remained lit for 1.4 seconds. For the first 0.7 seconds of this period, the target was one color and then turned to a different color. Subjects were instructed to reach the target about when its color changed. If the target changed location (shift condition), the subject was instructed to move toward the new target location. The shift occurred at 0.4 seconds with 50% probability. No specific instructions on movement speed, endpoint accuracy, or type of trajectory to be generated were given to the subject. All subjects performed a total of 1280 movements (640 movements from the central to the outer targets and 640 movements back). Three-minute rest breaks were given after every 160 movements. Only the movements from the central to the outer targets were analyzed. Subjects were allowed to practice until they were comfortable with the motor task.

C. Kinematic Data Analysis

Speed profiles of movements from the central to the outer targets were calculated as root-square of the sum of squared velocity components. Velocity components were obtained from the first-time derivatives of position data smoothed with a low-pass 12 Hz zero-phase FIR filter. Gaussian-shaped submovements were extracted from the movement speed profiles using a greedy algorithm as described in [7]. For each subject, submovements with the highest peak were selected from each movement trial (one submovement for the control and two submovements for the shift condition) and their parameters were calculated (onset, time to peak value, and offset).

D. EEG Data Analysis

EEG analysis was performed using the EEGLAB toolbox [17] for Matlab (MathWorks, Natick, MA). After re-referencing to the average reference, EEG data were high-pass filtered with a 1 Hz zero-phase FIR filter to remove offset and trend and downsampled at 128 Hz. Following removal of data sections containing artifacts identified via visual inspection, EEG data were further inspected for artifacts with a procedure based on Independent Component (IC) and dipole analysis as described in [17] [18]: IC scalp maps and frequency spectra were inspected, and ICs that displayed features indicative of artifacts were removed. Dipoles models were fit to the remaining components using the DIPFIT plug-in for EEGLAB and localized within a three-shell boundary element model of the Montreal Neurological Institute standard brain. Only the ICs whose dipoles resided within the brain volume of the head model and displayed less than 15% residual variance were retained. An average of 12±2.6 ICs per subject was retained. Cleaned EEG data were generated by back-projecting the retained ICs to the electrodes.

EEG activity was then epoched 200 ms prior to and 1400 ms after the presentation of the outer target or visual stimulus, for which linear de-trend and baseline correction procedures were applied. Epochs were aligned and averaged, separately for each condition (control or shift). ERPs were computed separately for each subject relative to the 200 ms pre-stimulus baseline. An average of 300.66±9.07 epochs and 317.33±26.35 epochs per subject was retained for the control and shift condition respectively. For each subject similarities among ERP topographical scalp maps at different time instants were quantified with Pearson's correlation coefficients.

III. RESULTS

A. Control Condition

Wrist speed profiles were similar across subjects, demonstrating single peak/bell-shaped characteristics (see Figure 2, left panel). The results of speed profiles submovement decomposition are presented in Table I. Submovement onsets were at 240.6±29.8 ms after stimulus onset (target presentation) and submovement peak values were reached at 424.16±43.01 ms after stimulus onset.
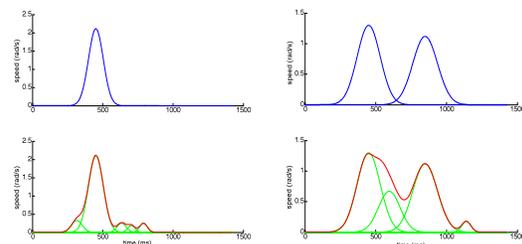

Figure 2: Speed profiles (red) and submovements (green) for the control (left) and shift (right) condition. The main submovements are defined as the submovement with the highest peaks (blue line), as detailed in Section II.

Figure 3, top shows typical ERP topographical scalp maps. Figure 4, left shows a typical ERP-image plot and signal for electrode C1 (over contralateral motor cortex). A slow negative potential was observed before target presentation (0 ms), followed by a positive potential (a feature enhanced by our signal processing technique) observed consistently across subjects at 197.9±18.01 ms (i.e. 226.3±27.12 ms prior to submovement peak) and by a negative potential.

B. Shift Condition

Movement was initially directed towards the first target and then changed direction and moved to the second target. Speed profiles displayed two main peaks, which corresponded to the movement towards the first and the second target (see Figure 2, right panel). Tables II and III summarize the results of submovement decomposition. The first and second submovements started respectively at 238.06±29.33 ms and 697.56±66.38 ms after stimulus onset; peak values for the first and second submovement were reached at 422.36±44.27 and 889.06±77.99 ms after stimulus onset, respectively.
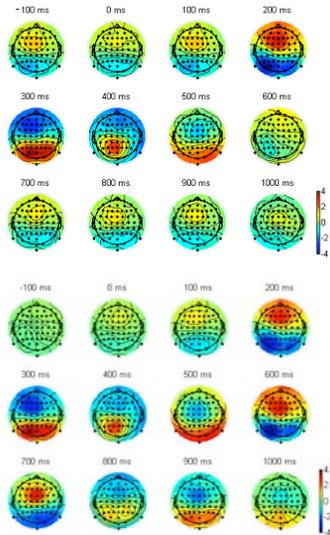

Figure 3: Topographical ERP scalp series for subject 1 for control (top) and shift (bottom) condition. Target was presented at 0 ms. At latencies 0-500 ms maps are similar. For the shift condition, maps at 600-1000 ms are very similar to maps at 200-500 ms.

In the pre-shift phase of the shift condition, topographical scalp maps were extremely similar to the maps associated to the control condition, indicating a similar underlying cortical activation (compare Figure 3, bottom with Figure 3, top). Pearson's correlation coefficients between the control and shift condition topographical scalp maps were 0.89±0.05 at 100 ms, 0.99±0.005 at 200 ms, 0.87±0.19 at 300 ms and 0.95± 0.03 at 400 ms, and for each subject correlations were highly significant. After target-shift occurred, scalp maps observed prior target-shift reoccurred. Specifically, the scalp maps we observed at 200 ms (similar for all subjects and occurring concurrently to the onset of the first submovement which averaged 238.06 ms) re-occurred at 600-700 ms depending on the subject (concurrent with the onset of the second submovement, which averaged 697.56 ms) as indicated by the high and significant positive correlations between scalp maps summarized in Table IV. The activation we observed at 300 ms re-occurred at 800-1100 ms, depending on the subject, as indicated by the high and significant positive correlations reported in Table V.
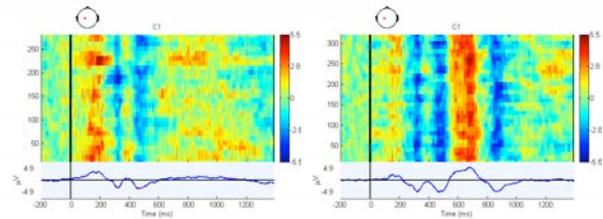

Figure 4: ERP image of channel C1 for the control (left) and shift (right) condition for subject 1. Amplitudes of EEG recordings during individual trials are shown. The vertical black line indicates onset of visual stimulus. The ERP signal is shown as the blue trace at the bottom of each panel.

	Subm Onset (ms)	Subm Peak (ms)	Subm Offset (ms)	Latency ERP Peak (ms)
Subj1	214.6 (49.2)	385.0 (50.9)	555.6 (70.0)	197.58
Subj2	234.0 (91.6)	417.3 (82.2)	601.7 (101.4)	229.86
Subj3	273.2 (68.0)	470.2 (58.8)	667.3 (85.6)	251.49

Table I: Latencies of submovement onset, peak, and offset for the control condition (mean, standard deviation). Latency of submovement peak compared to ERP positive peak is reported in the 5th column.

	Subm Onset (ms)	Subm Peak (ms)	Subm Offset (ms)	Latency ERP Peak (ms)
Subj1	208.0 (45.5)	381.5 (38.6)	555 (59.9)	217.44
Subj2	239.6 (87.6)	416.2 (68.0)	593.1 (81.8)	236.52
Subj3	266.6 (69.9)	469.4 (52.4)	672.3 (73.2)	258.47

Table II: Similar to Table I, for the shift condition. Data refer to the first submovement /ERP positive peak in the shift condition.

	Subm Onset (ms)	Subm Peak (ms)	Subm Offset (ms)	Latency ERP Peak (ms)
Subj1	677.0 (76.8)	874.0 (70.8)	1070.6 (98.8)	178.69
Subj2	643.9 (79.9)	825.8 (69.7)	1007.7 (86.2)	255.49
Subj3	771.8 (118.8)	967.4 (109.6)	1160.1 (119.3)	193.97

Table III: Similar to Table I, for the shift condition. Data refer to the second submovement /ERP positive peak in the shift condition.

The right panel of Figure 4 presents a typical ERP-image plot and signal for electrode C1. In the time interval 0-400 ms, the ERP was extremely similar to that recorded in the control condition (Figure 4, left). A positive ERP peak was observed consistently across subjects at 184.89±23.86 ms, i.e. 237.47±20.53 ms prior to the peak of the first kinematic submovement. After 400 ms (target shift), the ERP displayed a second positive peak, consistently across

subjects, at 679.68±102.45 ms, i.e. 209.38± 40.65 ms prior to the peak of the second submovement.

Time	Subj1	Subj2	Subj3	Time	Subj1	Subj2	Subj3
0s	0.98*	0.86*	0.91*	0s	-0.95*	-0.72*	-0.65*
0.1s	0.95*	0.71*	0.87*	0.1s	-0.97*	-0.48*	-0.75*
0.2s	1*	1*	1*	0.2s	-0.95*	-0.78*	-0.82*
0.3s	-0.95*	-0.78*	-0.82*	0.3s	1*	1*	1*
0.4s	-0.72*	-0.70*	-0.66*	0.4s	0.68*	0.26*	0.41*
0.5s	-0.65*	-0.37*	-0.35*	0.5s	0.74*	0.35*	0.35*
0.6s	0.97*	0.11	0.85*	0.6s	-0.96*	0.05	-0.65*
0.7s	0.87*	0.57*	0.24*	0.7s	-0.91*	-0.14	0.05
0.8s	-0.89*	0.33*	0.67*	0.8s	0.83*	-0.44*	-0.55*
0.9s	-0.91*	-0.15	-0.75*	0.9s	0.96*	-0.19	0.61*
1.0s	-0.81*	0.44*	-0.92*	1.0s	0.86*	-0.48*	0.80*
1.1s	0.94*	-0.78*	-0.97*	1.1s	-0.82*	0.63*	0.85*
1.2s	0.89*	-0.17	0.03	1.2s	-0.77*	0.63*	-0.04
1.3s	0.76*	0.35*	0.83*	1.3s	-0.79*	0.10	-0.72*
1.4s	0.95*	-0.54*	0.65*	1.4s	-0.94*	0.64*	-0.50*

*Table IV (left): Pearson's correlation coefficients between topographical scalp maps at 0.2 s and topographical scalp maps at 0-1.4 s, at 0.1 s intervals. * indicates statistical significance. Topographical scalp maps displayed at 0.2 s reappeared at 0.6 -0.7 s, as highlighted in gray.*

Table V (right): Pearson's correlation coefficients between topographical scalp maps at 0.3 s and topographical scalp maps at 0-1.4 s, at 0.1 s intervals. Maps displayed at 0.3 s reappeared at 0.8 s-1.1 s as highlighted in gray.

IV. DISCUSSION

How the CNS controls upper limb motion and modifies online motor commands to cope with changes that occur in the environment is not fully understood. A number of studies on unimpaired subjects have suggested that such complex motor behavior is constructed by superposing simpler movements or submovements that have a stereotyped shape and whose features are modulated by motor task demands (see for example [2]). Behavioral studies on stroke patients have corroborated this hypothesis by showing that the movements performed by stroke individuals display stereotyped and isolated submovements, which tend to blend as motor recovery progresses [8] [9]. Specifically, increases in motor smoothness displayed by stroke patients, both in the acute and chronic phase of recovery, can be explained by a submovement-based model [8]. Changes in submovement parameters have provided the basis for objectively quantifying both the quality of patients' movements and the level of motor generalization elicited by intervention [9]. Here we used a high-density EEG to investigate neural activation underlying motor corrections. We showed that the generation of each kinematic submovement was consistently accompanied by the occurrence of stereotyped cortical activation. First we showed that each submovement was

accompanied by the occurrence of stereotyped ERP topographical scalp maps. Specifically all subjects displayed similar scalp activations at 200-300 ms (onset of the first submovement in both conditions) and these activations reoccurred concurrently with the onset of the second submovement in the post-shift phase of the shift condition. Furthermore, we showed that positive ERP peaks recorded over the contralateral motor cortex (C1) were time-locked to kinematic submovement peaks. In particular, they occurred about 224 ms prior to kinematic submovement peaks. The steoreotyped character we observed in neural activations underlying submovements is consistent with the hypothesis that continuous movement is generated and controlled via discrete submovements.

REFERENCES

[1] R. S. Woodworth, "The accuracy of voluntary movements," *Psychol Rev* vol. 3, pp. 114, 1899.
[2] T. E. Milner, and M. M. Ijaz, "The effect of accuracy constraints on three-dimensional movement kinematics," *Neuroscience,* vol. 35, no. 2, pp. 365-74, 1990.
[3] R. C. Miall, D. J. Weir, and J. F. Stein, "Intermittency in human manual tracking tasks," *J Mot Behav,* vol. 25, no. 1, pp. 53-63, 1993.
[4] K. E. Novak, L. E. Miller, and J. C. Houk, "The use of overlapping submovements in the control of rapid hand movements," *Exp Brain Res,* vol. 144, no. 3, pp. 351-64, Jun, 2002.
[5] P. Morasso, and F. A. Mussa Ivaldi, "Trajectory formation and handwriting: a computational model," *Biol Cybern,* vol. 45, no. 2, pp. 131-42, 1982.
[6] T. E. Milner, "A model for the generation of movements requiring endpoint precision," *Neuroscience,* vol. 49, no. 2, pp. 487-96, 1992.
[7] H. I. Krebs, M. L. Aisen, B. T. Volpe *et al.*, "Quantization of continuous arm movements in humans with brain injury," *Proc Natl Acad Sci U S A,* vol. 96, no. 8, pp. 4645-9, Apr 13, 1999.
[8] B. Rohrer, S. Fasoli, H. I. Krebs *et al.*, "Movement smoothness changes during stroke recovery," *J Neurosci,* vol. 22, no. 18, pp. 8297-304, Sep 15, 2002.
[9] L. Dipietro, H. I. Krebs, S. E. Fasoli *et al.*, "Submovement changes characterize generalization of motor recovery after stroke," *Cortex,* vol. 45, no. 3, pp. 318-24, Mar, 2009.
[10] A. C. Lo, P. D. Guarino, L. G. Richards *et al.*, "Robot-Assisted Therapy for Long-Term Upper-Limb Impairment after Stroke," *N Engl J Med*, Apr 16, 2010.
[11] H. I. Krebs, N. Hogan, W. Hening *et al.*, "Procedural motor learning in Parkinson's disease," *Exp Brain Res,* vol. 141, pp. 425-37, 2001.
[12] E. Tunik, A. G. Feldman, and H. Poizner, "Dopamine replacement therapy does not restore the ability of Parkinsonian patients to make rapid adjustments in motor strategies according to changing sensorimotor contexts," *Parkinsonism Relat Disord,* vol. 13, no. 7, pp. 425-33, Oct, 2007.
[13] H. Poizner, A. G. Feldman, M. F. Levin *et al.*, "The timing of arm-trunk coordination is deficient and vision-dependent in Parkinson's patients during reaching movements," *Exp Brain Res,* vol. 133, no. 3, pp. 279-92, Aug, 2000.
[14] A. P. Georgopoulos, J. F. Kalaska, R. Caminiti *et al.*, "Interruption of motor cortical discharge subserving aimed arm movements," *Exp Brain Res,* vol. 49, no. 3, pp. 327-40, 1983.
[15] E. A. Henis, and T. Flash, "Mechanisms underlying the generation of averaged modified trajectories " *Biological Cybernetics,* vol. 72, no. 5, pp. 407-419, 1995.
[16] H. I. Krebs, B. T. Volpe, D. Williams *et al.*, "Robot-aided neurorehabilitation: a robot for wrist rehabilitation," *IEEE Trans Neural Syst Rehabil Eng,* vol. 15, no. 3, pp. 327-35, Sep, 2007.
[17] A. Delorme, and S. Makeig, "EEGLAB: an open source toolbox for analysis of single-trial EEG dynamics including independent component analysis," *J Neurosci Methods,* vol. 134, pp. 9-21, 2004.
[18] P. S. Hammon, S. Makeig, H. Poizner *et al.*, "Predicting Reaching Targets from Human EEG," *IEEE Signal Processing,* vol. 25, no. 1, pp. 69-77, 2008.